



# 1 Identifying ENSO Influences on Rainfall with Classification 2 Models: Implications for Water Resource Management of Sri 3 Lanka

4 Thushara De Silva M.<sup>1,3</sup>, George M. Hornberger<sup>1,2,3</sup>

5 <sup>1</sup>Department of Civil and Environmental Engineering, Vanderbilt University, Nashville, Tennessee, USA.

6 <sup>2</sup>Department of Earth and Environmental Science, Vanderbilt University, Nashville, Tennessee, USA. <sup>3</sup> Vanderbilt  
7 Institute for Energy and Environment, Vanderbilt University, Nashville, Tennessee, USA.

8 *Correspondence to:* Thushara De Silva M. ([thushara.k.de.silva@vanderbilt.edu](mailto:thushara.k.de.silva@vanderbilt.edu))

9 **Abstract.** Seasonal to annual forecasts of precipitation patterns are very important for water infrastructure  
10 management. In particular, such forecasts can be used to inform decisions about the operation of multipurpose  
11 reservoir systems in the face of changing climate conditions. Success in making useful forecasts often is achieved by  
12 considering climate teleconnections such as the El-Nino-Southern Oscillation (ENSO), Indian Ocean Dipole (IOD) as  
13 related to sea surface temperature variations. We present a statistical analysis to explore the utility of using rainfall  
14 relationships in Sri Lanka with ENSO and IOD to predict rainfall to Mahaweli and Kelani, river basins of the country.  
15 Forecasting of rainfall as classes; flood, drought and normal are helpful for the water resource management decision  
16 making. Results of these models give better accuracy than a prediction of absolute values. Quadratic discrimination  
17 analysis (QDA) and classification tree models are used to identify the patterns of rainfall classes with respect to ENSO  
18 and IOD indices. Ensemble modeling tool Random Forest is also used to predict the rainfall classes as drought and  
19 not drought with higher skill. These models can be used to forecast the areal rainfall using predicted climate indices.  
20 Results from these models are not very accurate; however, the patterns recognized are useful input to the water  
21 resources management and adaptation the climate variability of agriculture and energy sectors.

## 22 1 Introduction

23 The spatial and temporal uncertainty of water availability is one of the major challenges in water resource  
24 management. Understanding patterns and identifying trends in seasonal to annual precipitation are very important for  
25 water infrastructure management. In particular, forecasts that incorporate such information can be used to inform  
26 decisions about the operation of multipurpose reservoir systems in the face of changing climate conditions.

27 Success in making useful forecasts often is achieved by considering climate teleconnections such as the El-Nino-  
28 Southern Oscillation (ENSO) as related to sea surface temperature variations and air pressure over the globe using  
29 empirical data (Amarasekera et al., 1997; Denise et al., 2017; Korecha & Sorteberg, 2013; Seibert et al., 2017). Also,  
30 modes of variability of other tropical oceans can be related to regional precipitation (Dettinger and Diaz 2000; Eden  
31 et al. 2015; Maity and Kumar 2006; Malmgren et al. 2005; Ranatunge et al. 2003; Suppiah 1996; Roplewski &  
32 Halpert, 1996). For example, the effect of the Indian Ocean Dipole (IOD) is identified as independent of the ENSO  
33 effect (Eden et al., 2015). Pacific decadal oscillation (PDO), Atlantic multi-decadal mode oscillation (AMO), ENSO,  
34 and IOD teleconnections to precipitation have been found by many studies over the globe. Variations of precipitation  
35 in the United States are explained by ENSO, PDO and AMO (Eden et al., 2015; National Oceanic and Atmospheric



36 Administration, 2017; Ward, Eisner, Flo Rke, Dettinger, & Kummu, 2014), in African countries by ENSO, AMO and  
37 IOD (Reason et.al., 2006), and in South east Asian countries by ENSO: Indonesia (Lee, 2015; Nur'utami & Hidayat,  
38 2016), Thailand (Singhtrattna et.al., 2005), China (Cao et al., 2017; Ouyang et al., 2014; Qiu et.al., 2014). Australia  
39 (Bureau of Meteorology, 2012; Verdon & Franks, 2005), and central and south Asia (Gerlitz et al., 2016).

40 The impact of ENSO and IOD on the position of the intertropical convergence zone (ITCZ) has been identified as a  
41 primary factor driving south Asian tropical climate variations. South Asian countries get precipitation from two  
42 monsoons from the movements of ITCZ in boreal summer ( $2^{\circ}\text{N}$ ) and boreal winter ( $8^{\circ}\text{S}$ ). The South western monsoon  
43 (summer monsoon) is during June-August months and the North eastern monsoon (winter monsoon) is during  
44 December –February months (Schneider et.al, 2014). Climate teleconnections have been studied for summer  
45 monsoons (Singhtrattna et. al., 2005; Surendran et.al., 2015) and winter monsoons (Zubair & Ropelewski, 2006). A  
46 negative correlation of ENSO with Indian summer monsoon has been identified (Jha et al., 2016; Surendran et al.,  
47 2015).

48 The objective of this study is to explore the climate teleconnection to dual monsoons and inter monsoons. Water  
49 resource management decisions typically are based on precipitation throughout the year and it is extremely important  
50 to explore the possibility that rainfall might be related to teleconnection indices for which seasonal forecasts are  
51 available. Sri Lanka is a South Asian country that gets rainfall from two monsoons and two inter-monsoons. We  
52 explore ENSO and IOD climate teleconnection to Sri Lanka precipitation throughout the year. Past studies have  
53 identified climate teleconnection linking precipitation to climate indices for several months and monsoon seasons, and  
54 shown the importance of these for forecasting rainfall in river basins (Chandimala & Zubair, 2007; Chandrasekara et  
55 al., 2003). We extend these analyses across monsoon and inter-monsoon seasons.

56 Although rainfall anomalies may be correlated strongly with teleconnection indices, the scatter in the data can be  
57 large, making predictions from regression models have high uncertainty. However, water managers may act on  
58 information about whether rainfall is expected to be abnormally low or high. We investigate river basin rainfall  
59 teleconnections to climate indices with classification models. If reasonably accurate relationships can be developed,  
60 they will be useful for water resources management. For example, in Sri Lanka decisions about allocations of water  
61 for irrigation and hydropower could be improved with estimates of when low rainfall seasons are likely.

## 62 2 Methods

63 Sri Lanka is an island in the Indian Ocean (latitude  $5^{\circ}55' \text{ N} - 9^{\circ}50' \text{ N}$ , longitudes  $79^{\circ}40' \text{ E} - 81^{\circ}53' \text{ E}$ ). Mean annual  
64 rainfall varies from 880 mm to 5500 mm across the island. The rainfall distribution is determined by the monsoon  
65 system of the Indian Ocean interacting with the elevated land mass in the interior of the country. The country is divided  
66 into three climatic zones according to the rainfall distribution: wet zone (annual rainfall  $> 2500$  mm), intermediate  
67 zone ( $2500 \text{ mm} < \text{rainfall} < 1750$  mm) and dry zone (rainfall  $< 1750$  mm) (Department of Agriculture Sri Lanka,  
68 2017).

69 Sri Lanka, a water-rich country, has 103 river basins varying from  $9 \text{ km}^2$  to  $10448 \text{ km}^2$ . A large fraction of the water  
70 resources management infrastructure of the country is associated with the Mahaweli and Kelani river basins. The  
71 catchment areas of the Mahaweli and Kelani are  $10448 \text{ km}^2$  and  $2292 \text{ km}^2$  respectively. The two rivers start from the



72 central highlands. Mahaweli, the longest river, travels to the ocean 331 km in the eastern direction and the Kelani 145  
73 km in the western direction. Average annual discharge volume for the Mahaweli and Kelani basins are  $26368 \cdot 10^6 \text{m}^3$   
74 and  $8660 \cdot 10^6 \text{m}^3$  respectively (Manchanayake & Madduma Bandara, 1999). The Kelani river basin is totally inside the  
75 wet zone whereas the Mahaweli river basin migrates through all three climate zones (Figure 1).

76 The temporal pattern of rainfall in Sri Lanka can be divided into four seasons as follows.

77 (1) Generally low precipitation across the country from the Northeast monsoon (NEM), which gets most precipitation  
78 during January to February. The dry zone of the country gets significant precipitation from the NEM, while wet  
79 zone gets very little rainfall during this period.

80 (2) The whole country gets precipitation from the first inter-monsoon (FIM) during March to April months. However,  
81 rainfall during this period is not very high across the country.

82 (3) The highest precipitation for the country is from the South western monsoon (SWM) during May to September.  
83 However, only the wet zone gets high precipitation during this season.

84 (4) The whole country gets precipitation from the second inter-monsoon (SIM) during October to December.  
85 Generally, precipitation from SIM is higher than FIM.

86 The time period of NEM and SIM are generally considered as December to February and October to November  
87 respectively (Department of Meteorology Sri Lanka, 2017; Malmgren et.al, 2003; Ranatunge et al., 2003). However,  
88 considering the bulk amount of water received from the monsoon, we consider January and February as the period of  
89 NEM and October to December as the period of SIM.

90 Reflecting the rainfall seasons, the country has two agriculture seasons “Yala” (April - September) and  
91 “Maha”(October - March). Because the dry zone gets minimal precipitation during the SWM, the agricultural systems  
92 (165,000 ha) developed under the Mahaweli multipurpose project depend on irrigation water during the Yala season.  
93 The country depends on stored water to drive hydropower year round. The Mahaweli and Kelani hydropower plants  
94 of 810 MW and 335 MW capacity serve as peaking and contingency reserve power to the power system (Ceylon  
95 Electricity Board, 2015). Management of reservoir systems is done to cater both to irrigation and hydropower  
96 requirements.

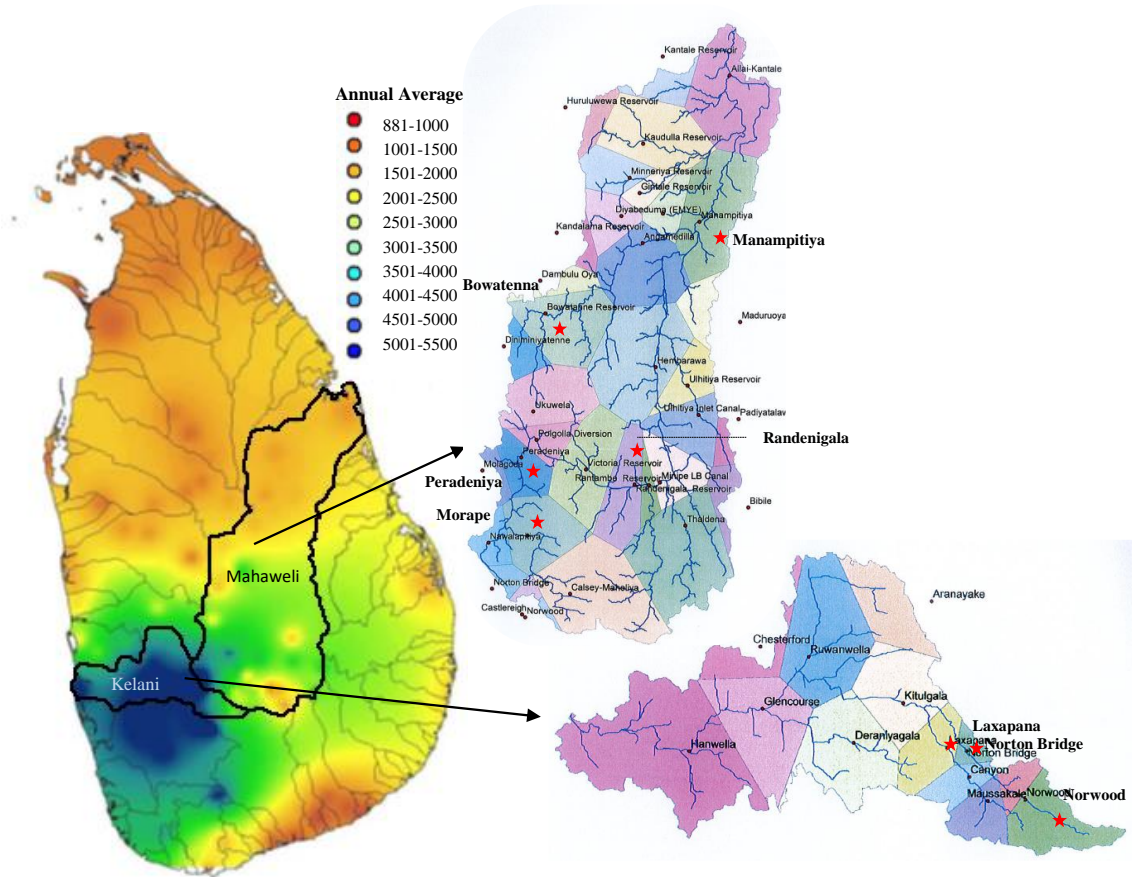


Figure 1: Mahaweli and Kelani river basins of Sri Lanka

97

98 **2.1 Sub Basin Rainfall (Areal Rainfall)**

99 Monthly rainfall data for years 1950-2013 are used for the study (Ceylon Electricity Board, 2017). River basin rainfall  
 100 was calculated using the Thiessen polygon method (Viessman, 2002). The Mahaweli river basin is divided into 16  
 101 Thiessen polygons and the Kelani river basin is divided into 11 Thiessen polygons (Figure 1). Eight sub-basins are  
 102 selected for analysis: Morape, Randenigala, Peradeniya, Manampitiya and Bowatenna represent the Mahaweli major  
 103 reservoir catchments and irrigation tanks, and Norton Bridge, Norwood and Laxapana represent the Kelani basin  
 104 reservoir catchments. The catchment of the major Mahaweli river reservoir cascade (Kotmale, Victoria, Randenigala,  
 105 Rantambe, Bowatenna) is represented by Morape and Peradeniya located in the wet zone and Randenigala and  
 106 Bowatenna located in the intermediate zone. The dry zone major irrigation catchments of the Mahaweli are represented  
 107 by Manampitiya. The Kelaniya reservoir cascade (Norton Bridge & Moussakele) catchments in the wet zone are  
 108 represented by Laxapana, Norton Bridge and Norwood sub-basins.



109 We calculate the rainfall for the four seasons, NEM, FIM, SWM and SIM for 64 years of historical data. Rainfall  
 110 anomalies are calculated by reducing the seasonal mean rainfall (Eq.(1)) and standardized anomalies are calculated  
 111 by dividing the rainfall anomalies by the standard deviation (SD) (Eq.(2)).

$$X_{ANM} = (X - \bar{X}_t) \quad \text{Eq.(1)}$$

$$X_{S\_ANM} = (X - \bar{X}_t)/SD_t \quad \text{Eq.(2)}$$

112 Where,  $\bar{X}_t$  is the average of seasonal rainfall,  $X_{ANM}$  is the rainfall anomaly and  $X_{S\_ANM}$  is the standardized rainfall  
 113 anomaly.

114 Standardized rainfall anomalies are divided into three classes as dry, average and wet (Table 1). A normality test for  
 115 the rainfall data classes is done using the Shapiro-Wilk test. If the rainfall data are not normally distributed, log (e),  
 116 square root or square functions are used to transform the data into normally distributed data sets.

117 Table 1: Rainfall anomaly classification

Class	Range
dry	Minimum $\leq X_{S\_ANM} < -0.5$
average	$-0.5 \leq X_{S\_ANM} < 0.5$
wet	$0.5 \leq X_{S\_ANM} \leq$ Maximum

118

## 119 2.2 ENSO & IOD Indices

120 The Multivariate ENSO Index (MEI) is based on sea-level pressure, zonal and meridional components of the surface  
 121 wind, sea surface temperature, surface air temperature, and total cloudiness fraction of the sky (National Oceanic and  
 122 atmospheric administration 2017). The Indian Ocean Dipole (IOD) is an oscillation of sea surface temperature in the  
 123 equatorial Indian ocean between Arabian sea and south of Indonesia (Bureau of Meteorology Australia, 2017). IOD  
 124 is identified as relevant to the climate of Australia (Power et al., 1999) and countries surrounded by the Indian ocean  
 125 in southern Asia (Chaudhari et al., 2013; Maity & Nagesh Kumar, 2006; Qiu et al., 2014; Surendran et al., 2015). The  
 126 Dipole Mode Index (DMI) is used to represent the IOD capturing the west and eastern equatorial sea surface  
 127 temperature gradient.

128 Data used for the analyses are MEI monthly data from years 1950 – 2013, (Climate indices, NOAA, 2017) and the  
 129 DMI monthly data from years 1950-2013 ( HadISST dataset, Japan Agency for Marine-Earth Science and Technology  
 130 2017). Averages of MEI and DMI values for four rainfall seasons are used for the statistical analysis.

## 131 2.3 Statistical Analyses

132 Seasonal values of MEI and DMI were used as the predictors to classify seasons into the three rainfall classes. The  
 133 total data set is divided into 75 % for training the model and 25 % for testing model performance. Quadratic  
 134 discriminant analysis (QDA) and classification trees were selected for the analyses. A random forest model also was  
 135 applied to investigate the reliability of a cross-validated statistical forecast tool based on an advance estimate of MEI  
 136 and DMI.



### 137            2.3.1      Quadratic Discriminant Analysis (QDA)

138      QDA assumes that observations from each class are drawn from a Gaussian distribution. Substituting a Gaussian  
139      density function of  $K^{\text{th}}$  class to Bayes theorem and taking the log values, the quadratic discriminant function is derived  
140      (James et.al., 2013; Löwe et.al., 2016) (Eq.(3))Eq.(3).

$$\delta_k(x) = -\frac{1}{2} (x - \mu_x)^T \Sigma_k^{-1} (x - \mu_x) + \log \pi_k \quad \text{Eq.(3)}$$

141      The covariance matrix ( $\Sigma_k$ ), mean ( $\mu_x$ ) and prior probability ( $\pi_k$ ) for each class are estimated from the training data  
142      set. These values are inserted into the discriminant function together with state variables and the corresponding class  
143      is selected according to the largest value of the function. The number of parameters to be estimated for the QDA model  
144      for  $K$  classes and  $p$  predictors are  $K \cdot p \cdot (p + 1) / 2$  values. The QDA model output is the probability that an  
145      observation of a climate category will fall into each of the rainfall classes.

### 146            2.3.2      Classification Tree model

147      For the classification tree model the predictor space is divided into non-overlapping regions ( $R_1 \dots R_j$ ). A classification  
148      tree predicts each observation as belonging to the most commonly occurring class of the training data regions (James  
149      et.al., 2013).

150      The Gini index ( $G$ ) is considered as the criterion for splitting into regions (James et.al., 2013).

$$G = \sum_{k=1}^K \hat{p}_{mk} (1 - \hat{p}_{mk}) \quad \text{Eq.(4)}$$

151      In Eq.(4),  $\hat{p}_{mk}$  represents the fraction of observations in the  $m^{\text{th}}$  class that belong to the  $k^{\text{th}}$  class. The Gini index is  
152      considered as a measure of node purity of the tree model, since small values of the index indicate that node has a  
153      higher number of observations from a single class. The complexity of trees is adjusted using a pruning process to  
154      produce more interpretable results.

155      Tree models give the probability that an observation falls into each of the three rainfall classes. The predicted class is  
156      assigned based on the highest probability. Tree models handle ties of probability values by randomly assigning the  
157      class.

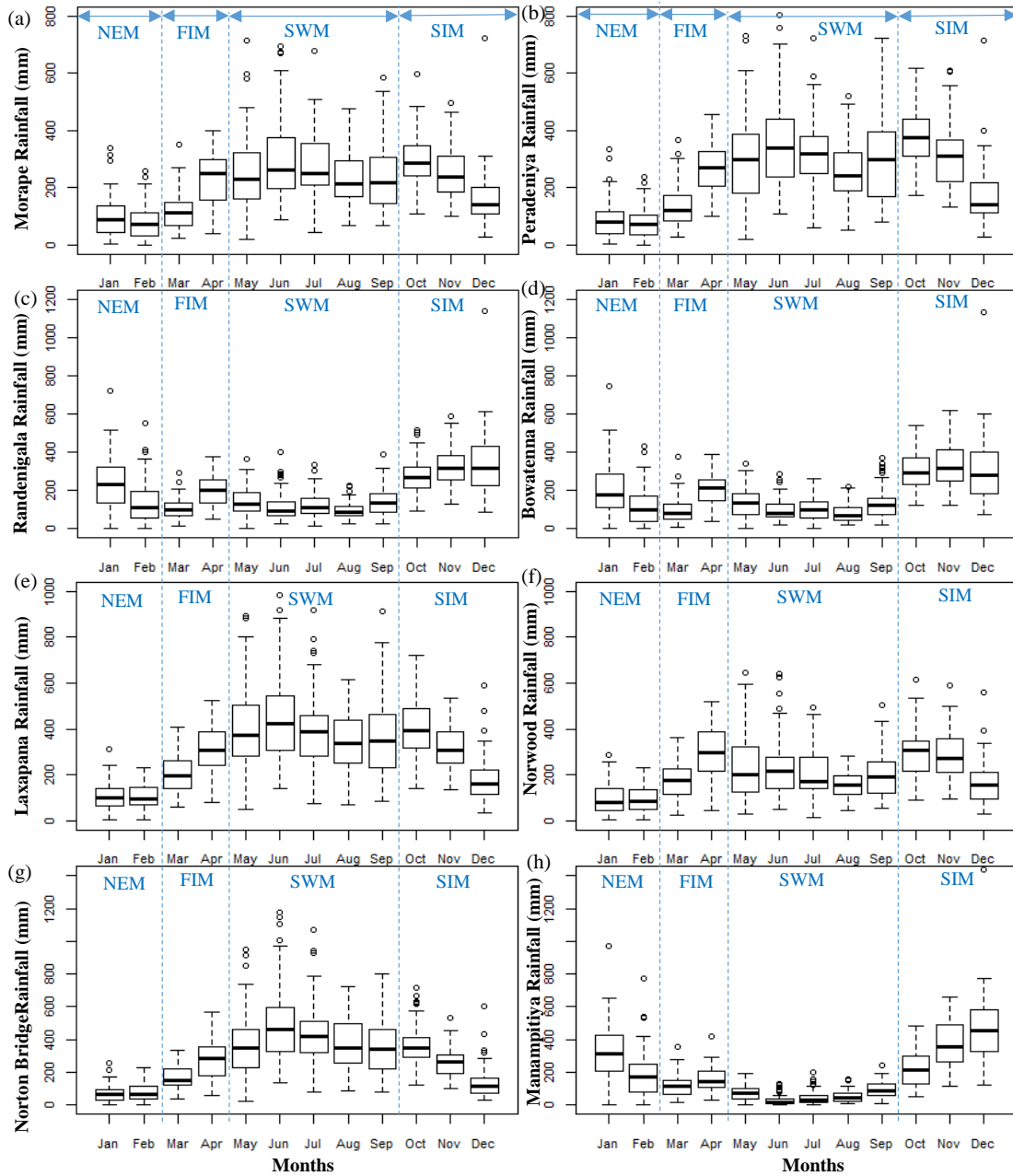
### 158            2.3.3 Random Forest

159      A random forest is an ensemble learning method used for classification and regression problems. The method is based  
160      on a multitude of decision trees based on training data with the final model as the mean of the ensemble (Breiman,  
161      2001). Individual trees are built on a random sample of the training data with several predictors from the total number  
162      of predictors. Individual trees are built from the bootstrapped training data set.

163



164 In a random forest model the importance of the variable is measured as the decrease in node impurity from the splits  
165 over the variable. This value is calculated by averaging the Gini index over the multitude of trees with a larger value  
166 indicating high importance of the predictor (James et.al., 2013).



167

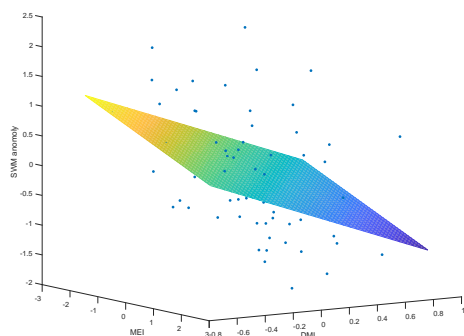
168 Figure 2: Sub basin Rainfall for (a) Morape, (b) Peradeniya, (c) Randenigala, (d) Bowatenna, (e) Laxapana (f)  
 169 Norwood, (g) Norton Bridge, and (h) Manampitiya.



### 170 3 Results

171 Monthly rainfall boxplots of eight sub basins over the year for 1950 - 2013 illustrate the seasonal and the spatial  
172 variation of rainfall patterns (Figure 2). The largest fraction of total rainfall in the dry zone occurs at the end of the  
173 SIM (December) and during the NEM (January - February) with correspondingly high variability whereas there is  
174 little rainfall in the dry zone during the SWM (May - September) with correspondingly little variability (Figure 2 (h)).  
175 The intermediate zone receives approximately 60% of total rainfall from the SIM and NEM. Although the variability  
176 of the rainfall is low in the intermediate zone, high rainfall can occur in all seasons (Figure 2 (c) and (d)). In the wet  
177 zone, a large portion of rainfall occurs in SWM and early months of SIM (October-November). High variability of  
178 wet zone rainfall is observed at the end of FIM (April), in the SWM (May-September), and at the start of SIM  
179 (October) (Figure 2 (a), (b), (e), (f) and (g)).

180 Similar to other investigators, we observe several strong correlations between rainfall anomalies and the climate  
181 indices (Table A.1, Appendix). For example, rainfall in the SWM is very important for stations in the wet zone of  
182 the country which is the source of a large amount of water stored in reservoirs. Correlation coefficients between  
183 SWM rainfall at Norton Bridge are negative and strong, -0.31 for MEI ( $p=0.01$ ) and -0.37 for DMI ( $p<0.01$ ). The  
184 strength of the correlation notwithstanding, the residuals from a regression model indicate that high uncertainty  
185 would attach to any forecast (Fig. 3). Thus, we are led to explore the efficacy of classification methods (Appendix).



186

187 Figure 3: Linear regression of rainfall anomaly on MEI and DMI. High values of MEI and DMI are associated with  
188 low values of rainfall.

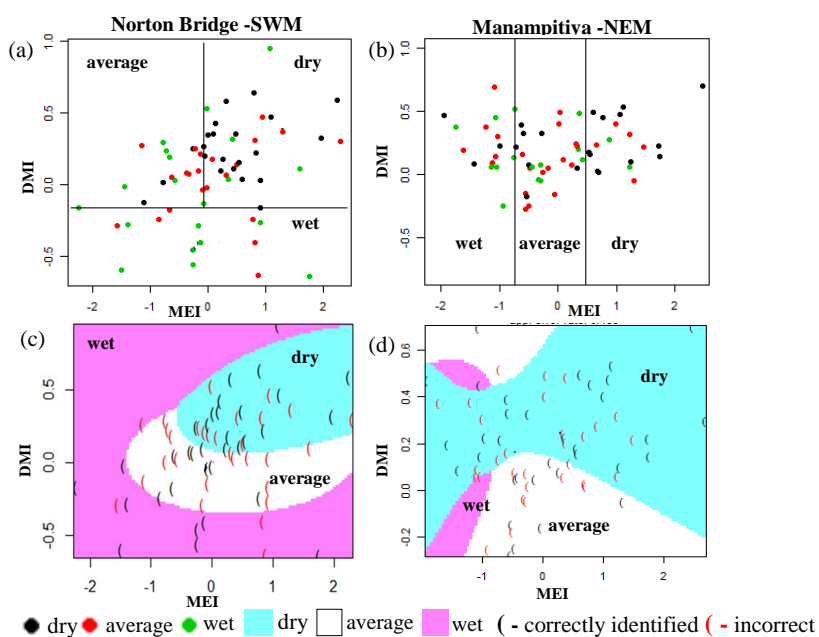
189 We present classification results for two sub-basins, one that has the highest rainfall during the NEM, Manampitiya,  
190 and one that has the highest rainfall for the SWM, Norton Bridge (Figure 4). Norton Bridge represents the areal rainfall  
191 of reservoir catchments in the wet zone and Manampitiya represents the rainfall that contributes to irrigation tanks in  
192 the dry zone. Results of other sub-basins are presented in the supplementary materials (Appendix).

193

194 The SWM is a season when the wet zone receives the bulk of rainfall. At Norton Bridge, the occurrences of the dry  
195 rainfall anomaly class in the SWM is seen to “clump” in the region of relatively high MEI and DMI. Both the  
196 classification tree and the QDA successfully identify the pattern (Fig. 4(a) and 4(c)) with an overall accuracy of 73 %,



197 19 and 16 correct out of 22 occurrences (Table 2). In the dry zone the NEM season is one of the most important for  
 198 rainfall. At Manampitiya, the MEI provides the primary variable in the classification, with the dry anomaly class being  
 199 correctly selected in 52 % by tree model and 95 % with the QDA model. The results suggest that it may be possible  
 200 to identify seasons when it is expected to be anomalously dry. The correct classification of “average” conditions likely  
 201 has less importance for water managers. We explored classification using two classes, “Dry” and “Not Dry.” In this  
 202 case, the classification model again correctly classifies 86 % of the anonymously dry cases and gets more than 69 %  
 203 of the “Not Dry” cases correct (Figure 5).



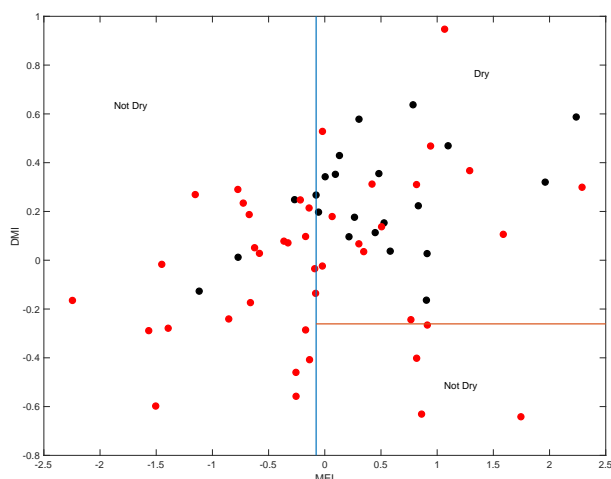
204

205

206

207

Figure 4: Norton Bridge and Manampitiya rainfall classes (dry, average, wet ) identified by ENSO and IOD phenomena. (a) Norton Bridge SWM rainfall classification tree model (b) Manampitiya NEM rainfall classification tree model (c) Norton Bridge SWM rainfall QDA



208

209 Figure 5: Classification tree for Norton Bridge SWM rainfall using two categories (dry and not dry)

210 Table 2: Classification model results. Highlighted cells indicate where there may be information content with  
 211 respect to forecasting either dry or wet anomaly classes as judged by a classification success rate of at least 2/3.

Season	Manampitiya			Norton Bridge		
	QDA Model			QDA Model		
	Dry	Normal	Wet	Dry	Normal	Wet
NEM	22/23	11/25	1/16	5/20	25/29	2/15
FIM	9/21	20/24	5/19	3/20	14/23	14/20
SWM	2/21	30/27	2/16	16/22	9/22	9/20
SIM	17/25	13/20	7/19	7/22	15/22	11/20
Season	Tree Model			Tree Model		
	Dry	Normal	Wet	Dry	Normal	Wet
	NEM	12/23	9/25	11/16	11/20	18/29
FIM	9/21	19/24	8/19	13/21	6/23	15/20
SWM	6/21	25/27	7/16	19/22	8/22	9/20
SIM	20/25	0/20	17/19	19/22	5/22	14/20

212

213 Classification trees are known to be unstable. That is, small changes in the observations can lead to large changes in  
 214 the decision tree. The random forest approach overcomes the issue by building a “bag” of trees from bootstrap samples.  
 215 The robustness of the model can then be checked by considering the “out-of-bag” error. The results of the random  
 216 forest indicate that predictions of three rainfall anomaly classes using MEI and DMI is not feasible (Table 3). The out-  
 217 of-bag error rate is close to two thirds, which for three categories is equivalent to a random selection.

218

219



220 Table 3: Results of random forest ensemble classification results

Season	Norton Bridge				Manampitiya			
	Dry	Normal	Wet	OOB Er	Dry	Normal	Wet	OOB Er
NEM	11/20	12/29	6/15	55%	14/23	10/25	5/16	55%
FIM	7/21	8/23	8/20	64%	10/21	11/24	6/19	58%
SWM	9/22	6/22	8/20	64%	6/21	17/27	5/16	56%
SIM	13/22	9/22	9/20	52%	15/25	8/20	7/19	53%

221

222 However, the results of the random forest for a classification as either “Dry” or “Not Dry” suggests that there may  
 223 be skill in such a prediction. The out-of-bag error rates for this case range from 22 % to 38 % for Norton Bridge and  
 224 Manampitiya (Table 3) and from 20 % to 39 % across all stations (Table A 6).

225 Table 4: Results of random forest ensemble classification results for two rainfall anomaly classes

Season	Norton Bridge			Manampitiya		
	Dry	Not dry	OOB Error	Dry	Not dry	OOB Error
NEM	9/20	36/44	30 %	13/23	33/41	28 %
FIM	5/21	35/43	38 %	8/21	35/43	33 %
SWM	9/22	32/42	36 %	5/16	34/43	39 %
SIM	10/22	36/42	28 %	16/25	34/39	22 %

226

#### 227 4 Discussion

228 Understanding seasonal rainfall variability across the spatially diverse Mahaweli and Kelani river basins is important  
 229 for irrigation and hydropower water planning. SWM and SIM are the key rainfall seasons for sub basins in the wet  
 230 zone (Norton Bridge, Morape, Peradeniya and Laxapana), delivering 80 % of annual rainfall (Figure 2 (a),(b),(e),(f)).  
 231 For the dry zone (Manampitiya) and intermediate zone (Randenigala, Bowatenna) sub basins, the major season is  
 232 SIM, which delivers more than 40 % of annual rainfall (Figure 2 (c),(d),(h)). The dry zone also gets rainfall during  
 233 the NEM (24 % of annual rainfall at Manampitiya) and the intermediate zone gets rainfall during the SWM (25 % -  
 234 30 % of annual rainfall at Randenigala and Bowatenna).

235 Climate teleconnection indices are related to rainfall anomalies observed during the two main growing seasons, Yala  
 236 and Maha. The Maha agriculture season (October-March) depends on rain from SIM and NEM. During El Nino events  
 237 rainfall increases for the first three months of the Maha season (SIM: October-December) (Fig. A 1, Fig. A 2, Fig. A  
 238 3, Fig. A 4) (Ropelewski and Halpert, 1995) and decreases during the last three months (NEM: January-March)(Figure  
 239 4 (b)). In Yala season (April-September), La-Nina events enhance the rainfall during SWM (Figure 4(a), (c), Fig. A  
 240 1, Fig. A 2, Fig. A 3, Fig. A 4)(Whitaker et.al, 2001). During El Nino events the SWM rainfall is reduced (Figure 4(a),  
 241 (c), Fig. A 5, Fig. A 6) (Zubair, 2003; Chandimala & Zubair, 2007; Chandrasekara et.al,2017). The El Nino impact  
 242 during the SWM is not as significant as it is during the NEM season (International Research Institute, 2017a). We



243 find, however, that there is an interaction between two teleconnection indices, MEI and IOD for SWM rainfall. During  
244 the Yala season there is a high probability of having a drought when both the IOD and MEI are positive (Figure 5).  
245 Also not having drought is probable when both the IOD and MEI are negative (Figure 5, Figure A 5, Fig. A 6).  
246 Classification of wet, average, and dry rainfall anomalies using the MEI and DMI indices is successful. For example,  
247 a dry SWM season for Norton Bridge (Table 2) and other wet-zone stations (Table A 3) is classified correctly with  
248 greater than 70 % accuracy with QDA and tree models. However, a random forest approach demonstrates that there  
249 is little skill in identifying a full wet-average-dry classification. However, a random forest model using only two  
250 rainfall categories shows more than 60 % accuracy in identifying “dry” and “not dry” classes of key rainfall seasons  
251 of the wet zone (Table 4, Table A 6). Similarly, for dry zone locations such as Manampitiya, the dry rainfall class  
252 identification for NEM and SIM seasons is about 60 % ( Table 4, Table A 6).  
253 Our statistical classification models can be combined with MEI and DMI forecasts to indicate the season-ahead  
254 expectation for rainfall. ENSO forecasts are available from the International Research Institute for Climate and Society  
255 (International Research Institute, 2017b) and IOD forecasts are available in the Bureau of Meteorology (BOM),  
256 Australian Government (Bureau of Meteorology, 2017). ENSO and IOD predictions are also associated with the  
257 uncertainty. Therefore, final forecast accuracy is a combination of the MEI, DMI forecast uncertainties and model’s  
258 accuracy rate in each class. Although overall prediction accuracy is not extremely high, a forecast of an anomalously  
259 low rainfall season can have value for risk-averse farmers (Cabrera et.a., 2007) and can guide plans for hydropower  
260 management (Block & Goddard, 2012).  
261 The electricity and agriculture sectors of Sri Lanka heavily rely on Mahaweli and Kelani river water resources so  
262 season ahead forecasts of abnormally low rainfall should be useful for decisions on adaptation measures. For example,  
263 water availability of the first three months of a growing season is important for crop selection and the extent of land  
264 to be cultivated. Hydropower planning and scheduling of maintenance of the power plants also can benefit from  
265 season-ahead forecasts. The damage that can occur due to incorrect rainfall forecasts in the agriculture and energy  
266 sectors can be minimized with emergency planning during the season, which is the usual practice.  
267 Although the accuracy of predicting low or not low seasonal rainfall is not very high, decisions based on forecasts that  
268 are improvements over climate averages should be an improvement over current practices. The accuracy of statistical  
269 models can be improved with longer records, which are important to train the classification models. Also, models can  
270 be fine-tuned for important shorter periods such as crop planting months and harvesting months for irrigation water  
271 planning.

## 272 5 Conclusion

273 ENSO and IOD phenomena teleconnections with river basin rainfall provide potentially useful information for water  
274 resource management. Relationships identified between teleconnection indices and river basin rainfall agree with other  
275 research findings. Prediction of seasonal rainfall classes from ENSO and IOD indices can inform water resources  
276 managers in reservoir operation planning for both hydropower and irrigation releases.

277  
278



279 **References:**

- 280 Amarasekera, K. N., Lee, R. F., Williams, E. R., and Eltahir, E. A. B.: ENSO and the natural variability in the flow  
281 tropical rivers. *Journal of Hydrology*, 200(1–4), 24–39, doi.org/10.1016/S0022-1694(96)03340-9, 1997.
- 282 Block, P., and Goddard, L.: Statistical and Dynamical Climate Predictions to Guide Water Resources in Ethiopia,  
283 138(June), 287–298., doi.org/10.1061/(ASCE)WR.1943-5452.0000181, 2012
- 284 Breiman, L.: Randomforest2001. *Machine Learning*, 45(1), 5–32., doi.org/10.1017/CBO9781107415324.004, 2001.
- 285 Bureau of Meteorology : Record-breaking La Niña events. *Bureau of Meteorology*, 26. available at :  
286 [www.bom.gov.au/climate/enso/history/La-Nina-2010-12.pdf](http://www.bom.gov.au/climate/enso/history/La-Nina-2010-12.pdf), 2012
- 287 Bureau of Meteorology : Indian Ocean, POAMA monthly mean IOD forecast., available at :  
288 [www.bom.gov.au/climate/enso/#tabs=Indian-Ocean](http://www.bom.gov.au/climate/enso/#tabs=Indian-Ocean), last access: 30 March 2017.
- 289 Cabrera, V. E., Letson, D., and Podesta, G.: The value of climate information when farm programs matter, 93, 25–  
290 42. doi.org/10.1016/j.agry.2006.04.005, 2007
- 291 Cao, Q., Hao, Z., Yuan, F., Su, Z., Berndtsson, R., Hao, J., and Nyima, T.: Impact of ENSO regimes on developing-  
292 and decaying-phase precipitation during rainy season in China. *Hydrology and Earth System Sciences*, 21(11),  
293 5415–5426, 2017
- 294 Ceylon Electricity Board.: Long Term Generation Expansion Plan 2015-2034 , Transmission and Generation  
295 Planning Branch Transmission Division Ceylon Electricity Board Sri Lanka, 2015
- 296 Ceylon Electricity Board.. River Basin Hydrology Data, System control branch Transmission Division. Sri Lanka,  
297 2017
- 298 Chandimala, J., and Zubair, L.: Predictability of stream flow and rainfall based on ENSO for water resources  
299 management in Sri Lanka. *Journal of Hydrology*, 335(3–4), 303–312. doi.org/10.1016/j.jhydrol.2006.11.024, 2007
- 300 Chandrasekara, S., Prasanna, V., and Kwon, H. H.: Monitoring Water Resources over the Kotmale Reservoir in Sri  
301 Lanka Using ENSO Phases. *Advances in Meteorology*, 2017, doi.org/10.1155/2017/4025964, 2017
- 302 Chaudhari, H. S., Pokhrel, S., Mohanty, S., & Saha, S. K.: Seasonal prediction of Indian summer monsoon in NCEP  
303 coupled and uncoupled model. *Theoretical and Applied Climatology*, 114(3–4), 459–477., doi.org/10.1007/s00704-  
304 013-0854-8, 2013
- 305 Denise, C., Rogers, W., and Beringer, J.: Describing rainfall in northern Australia using multiple climate indices,  
306 597–615., doi.org/10.5194/bg-14-597-2017, 2017
- 307 Department of Agriculture Sri Lanka.: Climate zones of Sri Lanka. available at:  
308 [www.doa.gov.lk/images/weather\\_climate/Climatezone.jpg](http://www.doa.gov.lk/images/weather_climate/Climatezone.jpg), last access: 7 November 2017.
- 309 Department of Meteorology Sri Lanka.: Climate of Sri Lanka. Retrieved November 7, 2017, available at:  
310 [www.meteo.gov.lk/index.php?option=com\\_content&view=article&id=94&Itemid=310&lang=en](http://www.meteo.gov.lk/index.php?option=com_content&view=article&id=94&Itemid=310&lang=en), 2017.
- 311 Dettinger, M. D., and Diaz, H. F.: Global Characteristics of Stream Flow Seasonality and Variability. *Journal of*  
312 *Hydrometeorology*, 1(4), 289–310., doi.org/10.1175/1525-7541(2000)001<0289:GCOSFS>2.0.CO;2, 2000.
- 313 Eden, J. M., Van Oldenborgh, G. J., Hawkins, E., and Suckling, E. B.: A global empirical system for probabilistic  
314 seasonal climate prediction. *Geoscientific Model Development*, 8(12), 3947–3973., doi.org/10.5194/gmd-8-3947-  
315 2015, 2015



- 316 Gerlitz, L., Vorogushyn, S., Apel, H., Gafurov, A., Unger-Shayesteh, K., & Merz, B.: A statistically based seasonal  
317 precipitation forecast model with automatic predictor selection and its application to central and south Asia.  
318 *Hydrology and Earth System Sciences*, 20(11), 4605–4623., doi.org/10.5194/hess-20-4605-2016, 2016
- 319 International Research Institute.: ENSO resources, El-Nino teleconnections & La-Nina teleconnections. Retrieved  
320 January 1, 2017, available at: [iri.columbia.edu/our-expertise/climate/enso/](http://iri.columbia.edu/our-expertise/climate/enso/), 2017a
- 321 International Research Institute.: IRI ENSO forecast. Retrieved January 1, 2017, available at: [iri.columbia.edu/our-expertise/climate/forecasts/enso/current](http://iri.columbia.edu/our-expertise/climate/forecasts/enso/current), 2017b
- 323 James, G., Witten, D., Hastie, T., and Tibshirani, R.: Springer Texts in Statistics An Introduction to Statistical  
324 Learning - with Applications in R., doi.org/10.1007/978-1-4614-7138-7, 2013
- 325 Japan Agency for Marine Earth Science and Technology.: SST/DMI data set. available at:  
326 [www.jamstec.go.jp/frcg/research/d1/iod/DATA/dmi.monthly.txt](http://www.jamstec.go.jp/frcg/research/d1/iod/DATA/dmi.monthly.txt), 2017.
- 327 Jha, S., Sehgal, V. K., Raghava, R., and Sinha, M.: Teleconnections of ENSO and IOD to summer monsoon and rice  
328 production potential of India. *Dynamics of Atmospheres and Oceans*, 76, 93–104,  
329 doi.org/10.1016/j.dynatmoce.2016.10.001, 2016.
- 330 Korecha, D., and Sorteberg, A.: Validation of operational seasonal rainfall forecast in Ethiopia. *Water Resources*  
331 *Research*, 49(11), 7681–7697. doi.org/10.1002/2013WR013760, 2013.
- 332 Lee, H.: General Rainfall Patterns in Indonesia and the Potential Impacts of Local Seas on Rainfall Intensity. *Water*,  
333 7(4), 1751–1769. doi.org/10.3390/w7041751, 2015
- 334 Löwe, R., Madsen, H., and McSharry, P.: Objective classification of rainfall in northern Europe for online operation  
335 of urban water systems based on clustering techniques. *Water (Switzerland)*, 8(3), doi.org/10.3390/w8030087, 2016.
- 336 Maity, R., and Nagesh Kumar, D.: Bayesian dynamic modeling for monthly Indian summer monsoon rainfall using  
337 El Nino-Southern Oscillation (ENSO) and Equatorial Indian Ocean Oscillation (EQUINOO). *Journal of*  
338 *Geophysical Research Atmospheres*, 111(7), 1–12. doi.org/10.1029/2005JD006539, 2006.
- 339 Malmgren, B. A., Hullugalla, R., Lindeberg, G., Inoue, Y., Hayashi, Y., & Mikami, T.: Oscillatory behavior of  
340 monsoon rainfall over Sri Lanka during the late 19th and 20th centuries and its relationships to SSTs in the Indian  
341 Ocean and ENSO. *Theoretical and Applied Climatology*, 89(1–2), 115–125. doi.org/10.1007/s00704-006-0225-9,  
342 2007.
- 343 Malmgren, B. A., Hulugalla, R., Hayashi, Y., and Mikami, T.: Precipitation trends in Sri Lanka since the 1870s and  
344 relationships to El Niño-southern oscillation. *International Journal of Climatology*, 23(10), 1235–1252.  
345 doi.org/10.1002/joc.921, 2003.
- 346 Manchanayake, P., and Madduma Bandara, C.: *Water Resources of Sri Lanka*, National Science Foundation, 1999.
- 347 National oceanic and atmospheric administration.: Cold & Warm Episodes by Season., available at:  
348 [www.cpc.ncep.noaa.gov/products/analysis\\_monitoring/ensostuff/ensoyears.shtml](http://www.cpc.ncep.noaa.gov/products/analysis_monitoring/ensostuff/ensoyears.shtml), last access: 30 March 2017.
- 349 National Oceanic and Atmospheric Administration.: El Nino Southern oscillation., available at:  
350 [http://www.esrl.noaa.gov/psd/enso/past\\_events.html](http://www.esrl.noaa.gov/psd/enso/past_events.html), 2017
- 351 Nur'utami, M. N., and Hidayat, R.: Influences of IOD and ENSO to Indonesian Rainfall Variability: Role of  
352 Atmosphere-ocean Interaction in the Indo-pacific Sector. *Procedia Environmental Sciences*, 33, 196–203.,  
353 doi.org/10.1016/j.proenv.2016.03.070, 2016.
- 354 Ouyang, R., Liu, W., Fu, G., Liu, C., Hu, L., and Wang, H.: Linkages between ENSO/PDO signals and



- 355 precipitation, streamflow in China during the last 100 years. *Hydrology and Earth System Sciences*, 18(9), 3651–  
356 3661. doi.org/10.5194/hess-18-3651-2014, 2014.
- 357 Power, S., Casey, T., Folland, C., Colman, A., and Mehta, V.: Inter-decadal modulation of the impact of ENSO on  
358 Australia. *Climate Dynamics*, 15(5), 319–324, doi.org/10.1007/s003820050284, 1999.
- 359 Qiu, Y., Cai, W., Guo, X., & Ng, B.: The asymmetric influence of the positive and negative IOD events on China's  
360 rainfall. *Scientific Reports*, 4, 4943, doi.org/10.1038/srep04943, 2014.
- 361 Ranatunge, E., Malmgren, B. A., Hayashi, Y., Mikami, T., Morishima, W., Yokozawa, M., and Nishimori, M.:  
362 Changes in the Southwest Monsoon mean daily rainfall intensity in Sri Lanka: Relationship to the El Niño-Southern  
363 Oscillation. *Palaeogeography, Palaeoclimatology, Palaeoecology*, 197(1–2), 1–14. doi.org/10.1016/S0031-  
364 0182(03)00383-3, 2003.
- 365 Reason, C. J. C., Landman, W., and Tennant, W.: Seasonal to decadal prediction of southern African climate and its  
366 links with variability of the Atlantic ocean. *Bulletin of the American Meteorological Society*, 87(7), 941–955.  
367 doi.org/10.1175/BAMS-87-7-941, 2006.
- 368 Ropelewski C.F. and Halpert M.S.: Quantifying Southern Oscillation-Precipitation Relationships. *Journal of*  
369 *Climate*, 1995
- 370 Schneider, T., Bischoff, T., and Haug, G. H.: Migrations and dynamics of the intertropical convergence zone.  
371 *Nature*, 513 (7516), 45–53. doi.org/10.1038/nature13636, 2014.
- 372 Seibert, M., Merz, B., and Apel, H.: Seasonal forecasting of hydrological drought in the Limpopo Basin: A  
373 comparison of statistical methods. *Hydrology and Earth System Sciences*, 21(3), 1611–1629., doi.org/10.5194/hess-  
374 21-1611-2017, 2017.
- 375 Singhrattna, N., Rajagopalan, B., Clark, M., and Kumar, K. K.: Seasonal forecasting of Thailand summer monsoon  
376 rainfall. *International Journal of Climatology*, 25(5), 649–664., doi.org/10.1002/joc.1144, 2005.
- 377 Singhrattna, N., Rajagopalan, B., Krishna Kumar, K., and Clark, M.: Interannual and interdecadal variability of  
378 Thailand summer monsoon season. *Journal of Climate*, 18(11), 1697–1708., doi.org/10.1175/JCLI3364.1, 2005.
- 379 Suppiah, R.: Spatial and temporal variations in the relationships between the southern oscillation phenomenon and  
380 the rainfall of Sri Lanka. *International Journal of Climatology*, 16(12), 1391–1407., doi.org/10.1002/(SICI)1097-  
381 0088(199612)16:12<1391, 1996.
- 382 Surendran, S., Gadgil, S., Francis, P. A., and Rajeevan, M.: Prediction of Indian rainfall during the summer  
383 monsoon season on the basis of links with equatorial Pacific and Indian Ocean climate indices. *Environmental*  
384 *Research Letters*, 10(9), 94004., doi.org/10.1088/1748-9326/10/9/094004, 2015.
- 385 Verdon, D. C., and Franks, S. W.: Indian Ocean sea surface temperature variability and winter rainfall: Eastern  
386 Australia., *Water Resources Research*, 41(9), 1–10. doi.org/10.1029/2004WR003845, 2005.
- 387 Ward, P. J., Eisner, S., Flo Rke, M., Dettinger, M. D., and Kummerow, M.: Annual flood sensitivities to el nintild;O-  
388 Southern Oscillation at the global scale. *Hydrology and Earth System Sciences*, 18(1), 47–66., doi.org/10.5194/hess-  
389 18-47-2014, 2014.
- 390 Whitaker, D. W., Wasimi, S. A., & Islam, S.: The El Niño southern oscillation and long-range forecasting of flows  
391 in the Ganges. *International Journal of Climatology*, 21(1), 77–87, 2001.
- 392 Zubair, L.: El Niño-southern oscillation influences on the Mahaweli streamflow in Sri Lanka. *International Journal*  
393 *of Climatology*, 23(1), 91–102. doi.org/10.1002/joc.865, 2003.



394 Zubair, L., and Ropelewski, C. F.: The strengthening relationship between ENSO and northeast monsoon rainfall  
 395 over Sri Lanka and southern India. *Journal of Climate*, 19(8), 1567–1575., doi.org/10.1175/JCLI3670.1, 2006.

396

## 397 **Appendix: Identifying ENSO Influences on Rainfall with Classification**

### 398 **Models: Implications for Water Resource Management of Sri Lanka**

399 Correlation coefficients between rainfall anomalies and MEI and DMI are negative for the NEM, FIM and SWM  
 400 seasons and positive for the SIM season. Rainfall anomalies correlations to the DMI are not stronger as the correlations  
 401 to the MEI. However, there are strong correlations for the anomalies of major monsoons to the sub basins and DMI  
 402 values. For example, wet sub basins (Morape, Peradeniya, Laxapana, Norwood, Norton Bridge) have high correlation  
 403 coefficient between SWM rainfall anomalies and DMI, while dry zone (Manampitiya) and intermediate zone  
 404 (Randenigala, Bowatenna) sub basins have high correlation coefficient between NEM and SIM rainfall anomalies.

405 Table A. 1: Correlation between rainfall anomalies and MEI, DMI indices. High correlation coefficients are  
 406 highlighted.

<b>Rainfall</b>	<b>Morape</b>		<b>Peradeniya</b>		<b>Randenigala</b>		<b>Bowatenna</b>	
Month	MEI	DMI	MEI	DMI	MEI	DMI	MEI	DMI
NEM	<b>-0.35</b>	-0.09	<b>-0.38</b>	-0.11	<b>-0.30</b>	-0.11	<b>-0.35</b>	<b>-0.20</b>
FIM	<b>-0.28</b>	-0.11	<b>-0.27</b>	-0.06	<b>-0.29</b>	-0.04	<b>-0.23</b>	-0.02
SWM	<b>-0.35</b>	<b>-0.29</b>	<b>-0.35</b>	<b>-0.31</b>	-0.17	<b>-0.24</b>	-0.18	-0.12
SIM	<b>0.21</b>	0.12	0.17	0.09	<b>0.37</b>	<b>0.35</b>	<b>0.35</b>	<b>0.36</b>
<b>Rainfall</b>	<b>Laxapana</b>		<b>Norwood</b>		<b>Norton Bridge</b>		<b>Manampitiya</b>	
Month	MEI	DMI	MEI	DMI	MEI	DMI	MEI	DMI
NEM	<b>-0.27</b>	-0.01	<b>-0.28</b>	-0.04	<b>-0.32</b>	-0.01	<b>-0.26</b>	<b>-0.16</b>
FIM	<b>-0.28</b>	-0.07	<b>-0.27</b>	-0.13	<b>-0.18</b>	-0.08	<b>-0.20</b>	-0.14
SWM	<b>-0.30</b>	<b>-0.31</b>	<b>-0.21</b>	<b>-0.24</b>	<b>-0.31</b>	<b>-0.37</b>	-0.07	-0.03
SIM	0.10	0.08	<b>0.29</b>	<b>0.28</b>	0.02	-0.15	<b>0.45</b>	<b>0.51</b>

407

408 Classification methods classification tree models, random forest and quadratic discriminant analysis identify the  
 409 relationship between standardized rainfall anomaly classes (dry, average, wet) and MEI and DMI values (Figure A 1,  
 410 Figure A 2, Figure A 3, Figure A 4). Positive values of MEI and DMI values resulted dry or average rainfall class for  
 411 the NEM, FIM and SWM seasons. However, for SIM rainfall has wet or average class for the positive values of MEI  
 412 and DMI. Accuracy of model result are high for the dominant monsoon rainfall seasons of each sub basin (Table A.  
 413 2, Table A. 3, Table A. 4). Ensemble model approach with random forest has given comparatively lower out-of-bag  
 414 error rate for the dominant monsoons' rainfall anomaly classification (Table A. 4). For example, wet zone sub basins  
 415 such as Norton Bridge, Norwood, Laxapana, Peradeniya and Morape random forest error rate is lower for the SWM  
 416 and SIM seasons. Same as, dry and intermediate sub basins Manampitiya, Randenigala and Bowatenna NEM and SIM  
 417 rainfall classes accuracy rate is high than other rainfall seasons. Also all three models have higher accuracy rate in



418 identifying dry events and error rate of identifying wet and dry class also less 15 % (Table A. 2, Table A. 3, Table A.  
419 4). Further analysis of two rainfall classes dry and not dry rainfall classes are identified relevant to the MEI and DMI  
420 values with classification tree and random forest methods (Figure A 5, Figure A 6). Classification tree models for two  
421 classes have higher accuracy rate as 65 % - 84 % for eight sub basins (Table A. 5). Random forest out-of-bag error  
422 for two classes models are vary between 20%-39% and shows higher skill in identifying rainfall classes for major  
423 monsoons of the sub basins (Table A. 6). MEI shows higher variable importance of identifying the rainfall classes  
424 compare to the DMI values. Specially, for NEM and SIM which are important to the dry zone sub basins importance  
425 of MEI is high in the classification. However, some of the wet zone sub basins shows equal importance of DMI  
426 variable in identifying two rainfall classes in FIM and SWM (Figure A 7).

427

428

429

430

431

432

433

434

435

436

437

438

439

440

441

442

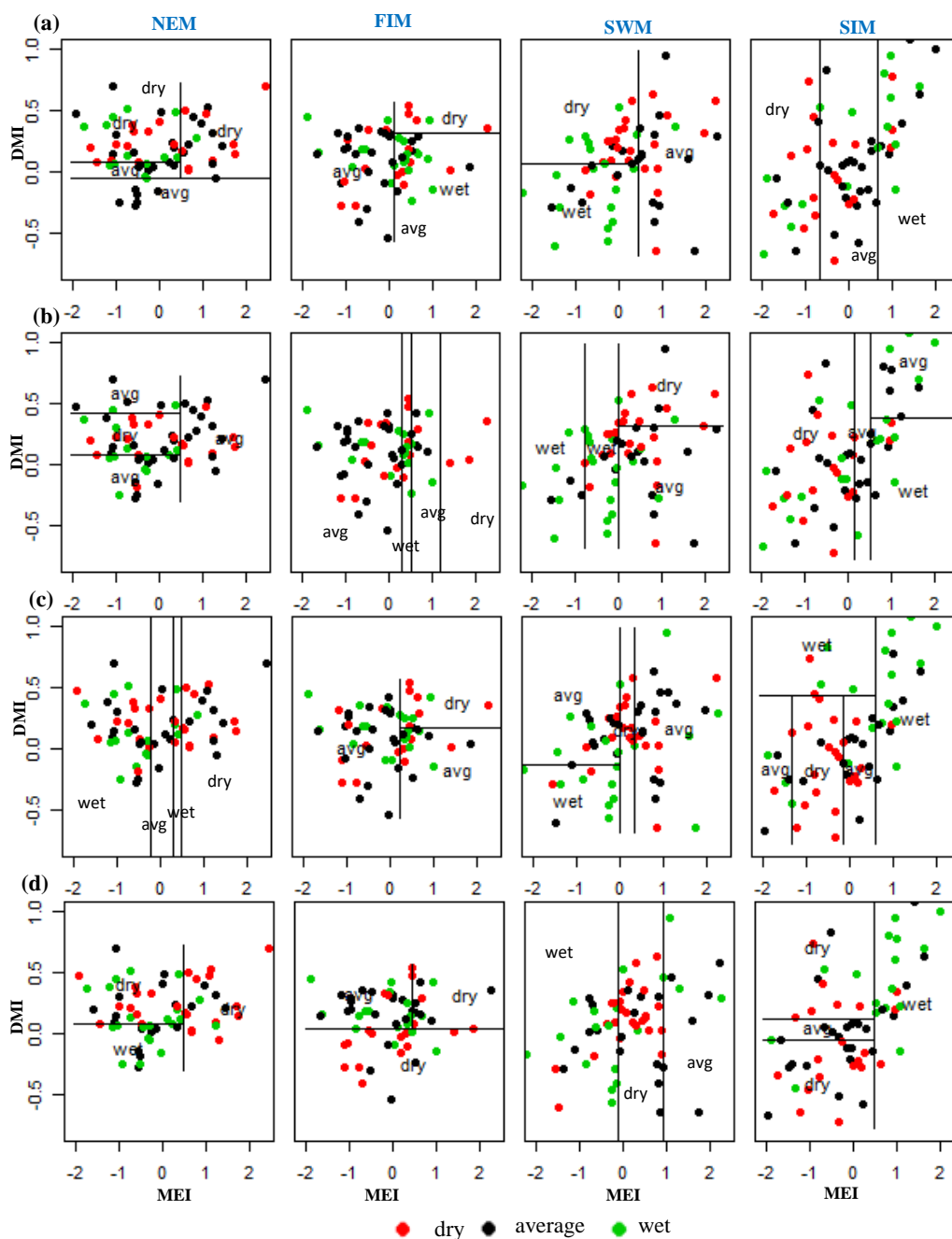
443

444

445

446

447

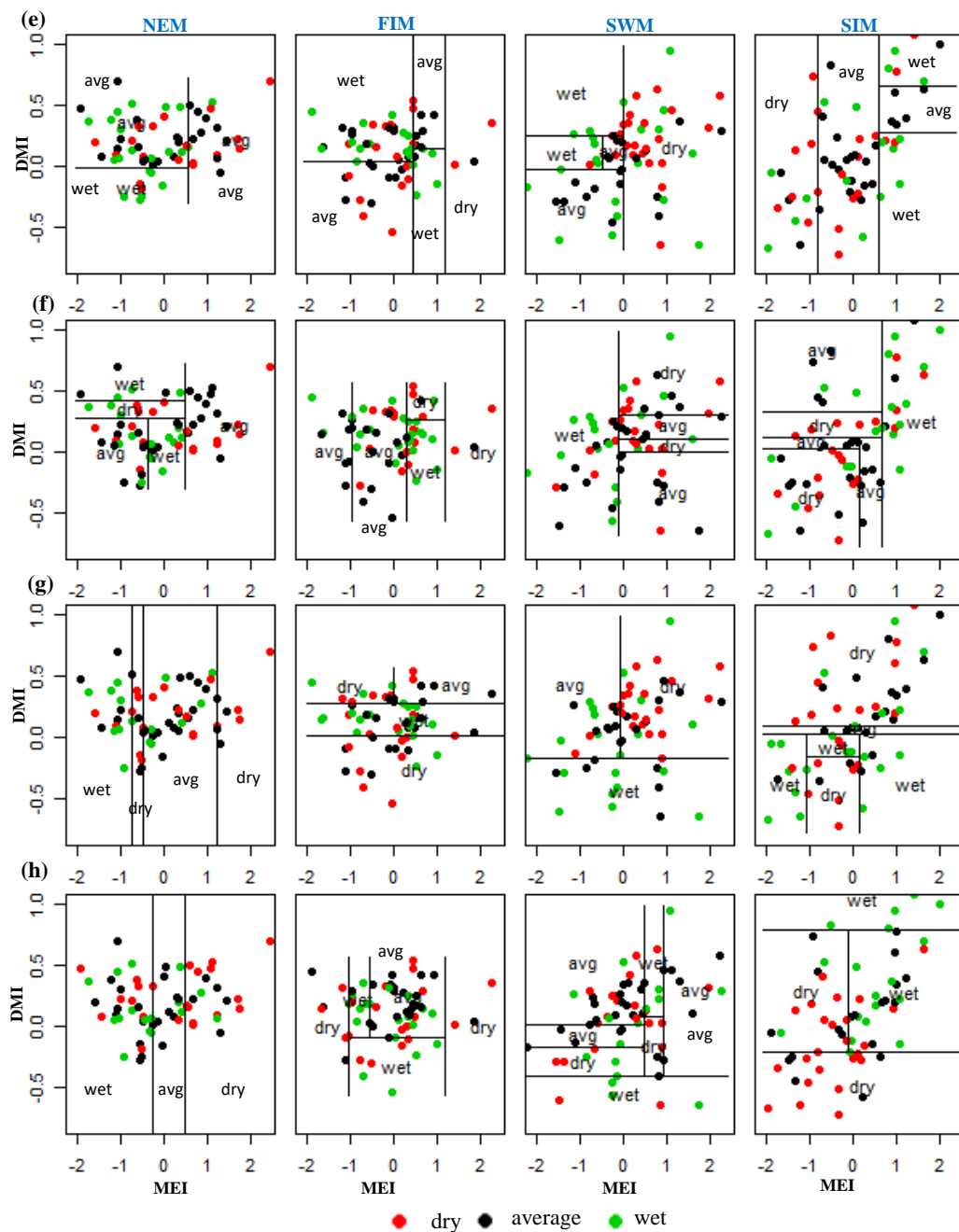


448

449

450

Figure A 1: Identifying relationships between three rainfall classes (dry, average, wet) and MEI and DMI values using classification tree models. (a) Morape (b) Peradeniya (c) Randenigala (d) Bowatenna



451

452

Figure A 2: Identifying relationships between three rainfall classes (dry, average, wet) and MEI and DMI values using classification tree models. (e)Laxapana (f)Norwood (g)Norton Bridge (h)Manampitiya

453



454 Table A. 2: Classification tree model results. Highlighted cells indicate where there may be information content with  
 455 respect to forecasting either dry or wet anomaly classes

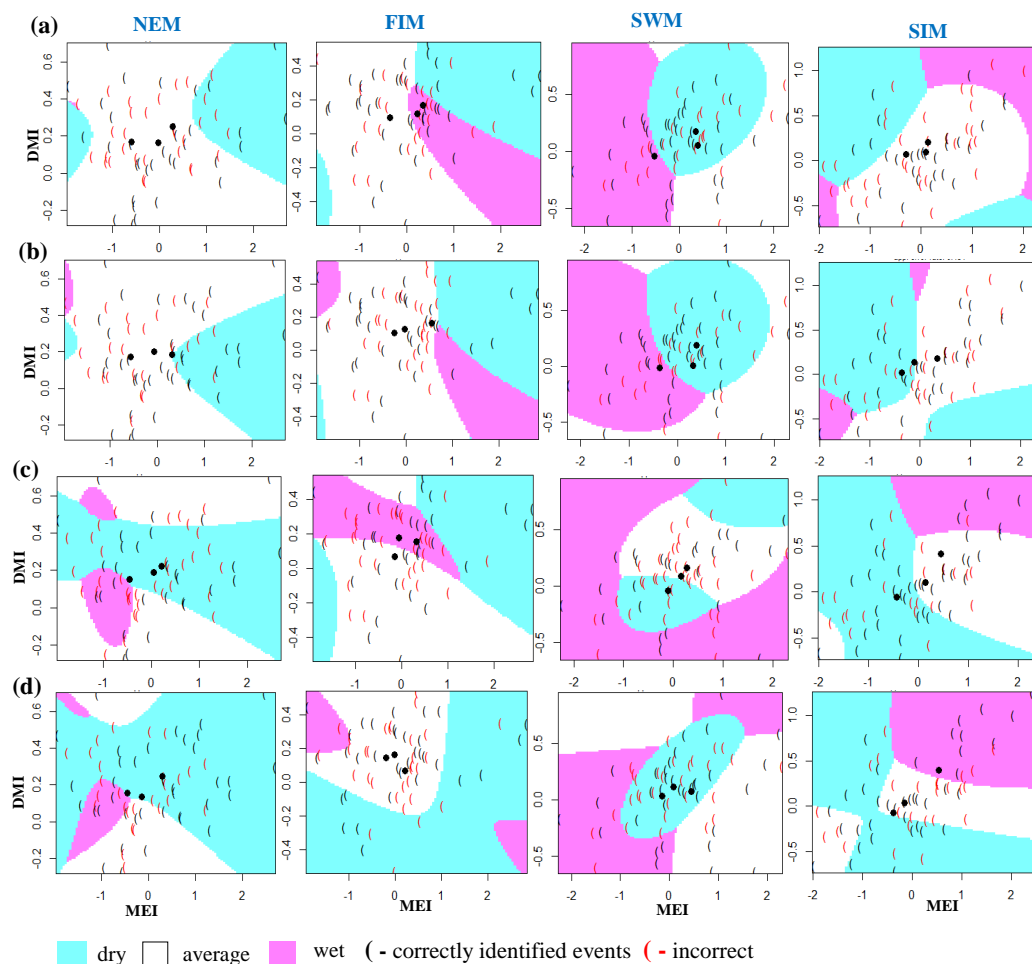
Season	Morape			Peradeniya		
	Dry	Normal	Wet	Dry	Normal	Wet
NEM	21/21	13/29	0/14	10/20	24/31	0/13
FIM	5/19	19/25	12/20	5/20	28/28	6/16
SWM	12/24	13/21	12/19	9/23	11/19	18/22
SIM	8/19	18/28	9/17	12/25	16/19	5/20
Season	Randenigala			Bowatenna		
	Dry	Normal	Wet	Dry	Normal	Wet
NEM	11/24	11/25	12/15	24/24	12/19	0/21
FIM	8/20	24/25	3/19	17/21	17/25	0/18
SWM	8/21	23/24	8/19	18/25	6/21	12/18
SIM	14/24	11/21	15/19	17/21	9/26	13/17
Season	Laxapana			Norwood		
	Dry	Normal	Wet	Dry	Normal	Wet
NEM	0/19	24/24	6/21	4/19	22/28	10/17
FIM	2/20	14/26	18/18	7/19	19/21	12/24
SWM	19/23	14/20	8/21	10/20	14/27	11/17
SIM	8/21	22/26	9/17	16/20	15/25	11/19
Season	Norton Bridge			Manampitiya		
	Dry	Normal	Wet	Dry	Normal	Wet
NEM	11/20	18/29	8/15	12/23	9/25	11/16
FIM	13/21	6/23	15/20	9/21	19/24	8/19
SWM	19/22	8/22	9/20	6/21	25/27	7/16
SIM	19/22	5/22	14/20	20/25	0/20	17/19

456

457

458

459



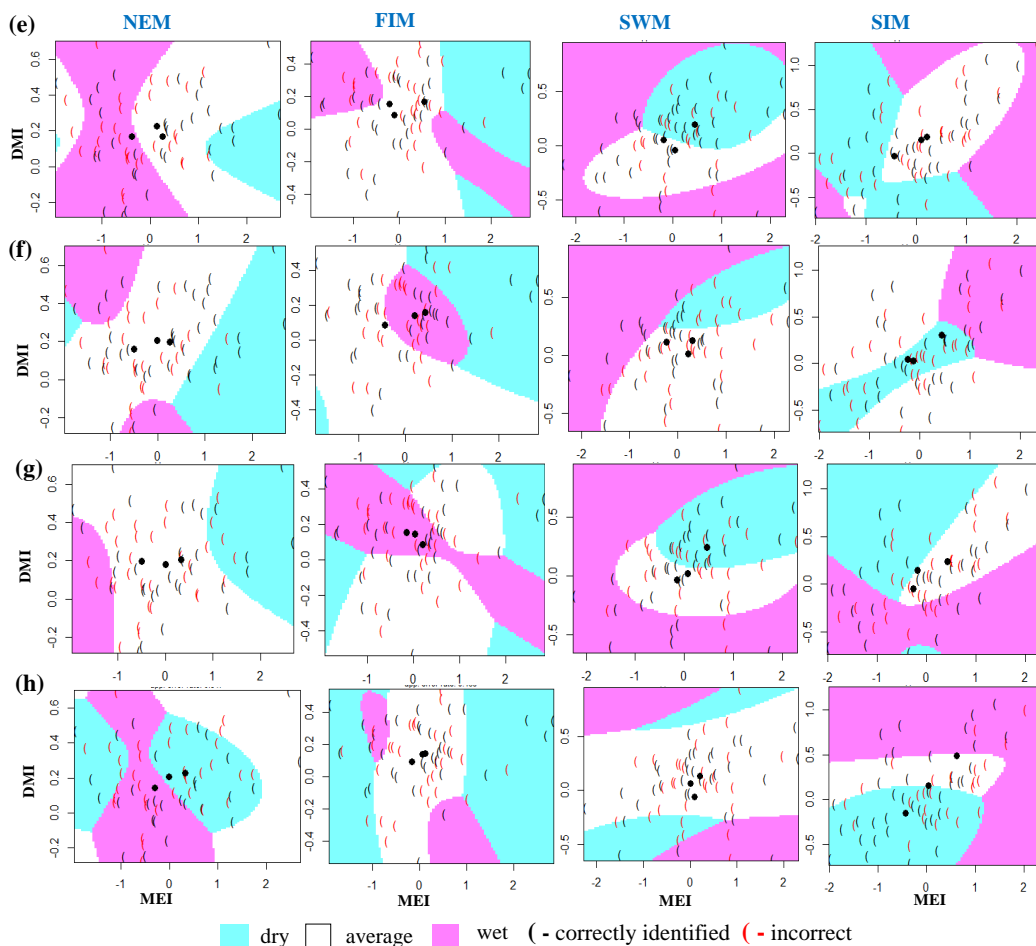
460

461

462

463

Figure A 3: Identifying relationships between three rainfall classes (dry, average, wet) and MEI and DMI values using QDA models.(a) Morape (b) Peradeniya (c) Randenigala (d) Bowatenna



464

465 Figure A: Identifying relationships between three rainfall classes (dry, average, wet) and MEI and DMI values  
 466 using classification tree models. (e) Laxapana (f) Norwood (g) Norton Bridge (h) Manampitiya

467

468

469

470

471

472

473

474



475 Table A. 3: Classification QDA model results. Highlighted cells indicate where there may be information content  
 476 with respect to forecasting either dry or wet anomaly classes

Season	Morape			Peradeniya		
	Dry	Normal	Wet	Dry	Normal	Wet
NEM	6/21	28/29	0/14	10/20	28/31	0/13
FIM	7/19	22/25	9/20	5/20	28/28	2/16
SWM	19/24	6/21	13/19	20/23	6/19	13/22
SIM	5/19	26/28	2/17	13/25	16/19	4/20
Season	Randenigala			Bowatenna		
	Dry	Normal	Wet	Dry	Normal	Wet
NEM	17/24	8/25	4/15	24/24	9/19	3/21
FIM	8/20	13/25	12/19	9/21	23/25	1/18
SWM	4/21	13/24	8/19	19/25	7/21	8/18
SIM	19/24	16/21	6/19	13/21	15/26	10/17
Season	Laxapana			Norwood		
	Dry	Normal	Wet	Dry	Normal	Wet
NEM	4/19	15/24	14/21	8/19	23/28	6/17
FIM	4/20	22/26	8/18	6/19	16/21	13/24
SWM	20/23	13/20	10/21	6/20	19/27	8/17
SIM	9/21	22/26	3/17	11/20	13/25	8/19
Season	Norton Bridge			Manampitiya		
	Dry	Normal	Wet	Dry	Normal	Wet
NEM	5/20	25/29	2/15	22/23	11/25	1/16
FIM	3/20	14/23	14/20	9/21	20/24	5/19
SWM	16/22	9/22	9/20	2/21	26/27	6/16
SIM	7/22	15/22	11/20	17/25	13/20	7/19

477  
 478  
 479  
 480  
 481  
 482  
 483  
 484  
 485  
 486



487 Table A. 4: Random forest model results. Highlighted cells indicate where there may be information content with  
 488 respect to forecasting either dry or wet anomaly classes

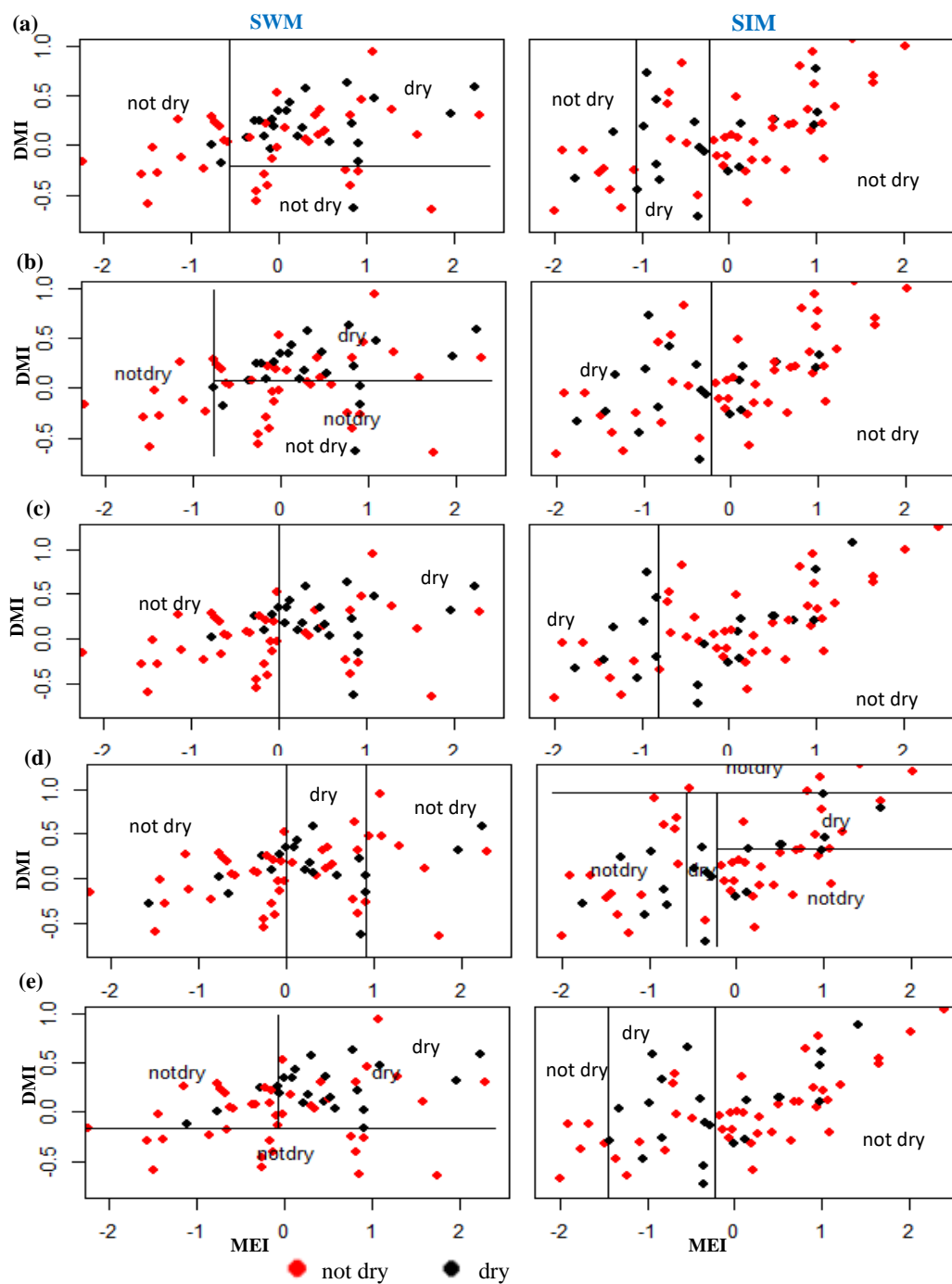
Season	Morape			Peradeniya		
	Dry	Normal	Wet	Dry	Normal	Wet
NEM	12/21	12/29	5/14	9/20	17/31	5/13
FIM	8/19	14/25	10/20	7/20	17/28	6/16
SWM	11/24	6/21	11/19	11/23	1/19	13/22
SIM	8/19	16/28	2/17	5/25	9/19	6/20
Season	Randenigala			Bowatenna		
	Dry	Normal	Wet	Dry	Normal	Wet
NEM	10/24	8/25	4/15	16/24	6/19	11/21
FIM	9/20	8/25	8/19	16/21	14/25	4/18
SWM	9/21	14/24	6/19	14/25	7/21	5/18
SIM	15/24	6/21	7/19	3/21	14/26	11/17
Season	Laxapana			Norwood		
	Dry	Normal	Wet	Dry	Normal	Wet
NEM	3/19	11/24	9/21	9/19	16/28	8/17
FIM	1/20	18/26	1/18	8/19	10/21	12/24
SWM	19/23	9/20	4/21	6/20	15/27	4/17
SIM	10/21	12/26	3/17	8/20	14/25	8/19
Season	Norton Bridge			Manampitiya		
	Dry	Normal	Wet	Dry	Normal	Wet
NEM	11/20	12/29	6/15	14/23	10/25	5/16
FIM	7/21	8/23	8/20	10/21	11/24	6/19
SWM	9/22	6/22	8/20	6/21	17/27	5/16
SIM	13/22	9/22	9/20	15/25	8/20	7/19

489

490

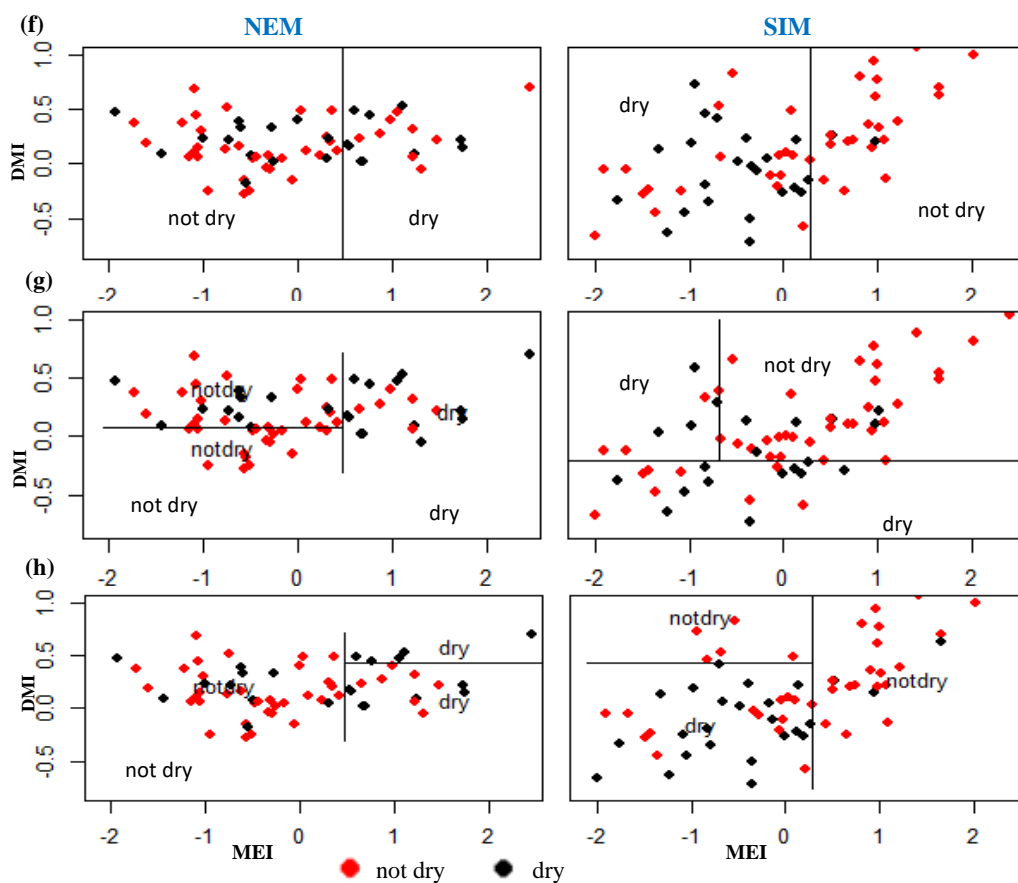
491

492



493

Figure A 5: Identifying relationships between two rainfall classes (dry, not dry) and MEI and DMI values using classification tree models for wet zone sub basins for SWM and SIM seasons. (a) Morape (b) Peradeniya (c) Laxapana (d) Norwood (e) Norton Bridge



494

495 Figure A 6: Identifying relationships between two rainfall classes (dry, not dry) and MEI and DMI values using  
 496 classification tree models for dry and intermediate zone sub basins for NEM and SIM seasons. (a) Randenigala (b)  
 497 Bowatenna (c) Manampitiya

498

499 Table A. 5: Classification tree model results for major rainfall season to the sub basins.

Season	Morape		Peradeniya		Laxapana		Norwood		Norton Bridge	
	Dry	Not dry	Dry	Not dry	Dry	Not dry	Dry	Not dry	Dry	Not dry
SWM	21/24	22/40	18/23	26/41	19/23	27/41	12/20	34/44	19/22	29/42
SIM	10/19	39/45	12/19	30/45	8/21	36/43	11/20	38/44	13/22	36/42
Season	Randenigala		Bowatenna		Manampitiya					
	Dry	Not dry	Dry	Not dry	Dry	Not dry				
NEM	11/24	31/40	14/24	34/40	13/23	34/41				
SIM	23/24	22/40	15/21	32/43	22/25	26/39				

500



501

502 Table A. 6: Random forest model results.

Season	Morape			Peradeniya		
	Dry	Not dry	OOB Error	Dry	Not dry	OOB Error
NEM	10/21	33/43	33%	8/20	34/44	34%
FIM	5/19	36/45	36%	6/20	37/44	33%
SWM	11/24	29/40	38%	11/23	28/41	39%
SIM	5/19	39/45	33%	5/19	37/45	34%
Season	Randenigala			Bowatenna		
	Dry	Not dry	OOB Error	Dry	Not dry	OOB Error
NEM	8/24	31/40	39%	15/24	33/40	25%
FIM	6/20	39/44	30%	13/21	38/43	20%
SWM	7/21	38/43	30%	11/25	29/39	38%
SIM	13/24	31/40	31%	6/21	35/43	36%
Season	Laxapana			Norwood		
	Dry	Not dry	OOB Error	Dry	Not dry	OOB Error
NEM	8/20	37/45	30%	10/19	39/45	23%
FIM	7/20	37/44	31%	8/19	39/45	26%
SWM	12/23	27/41	39%	7/20	37/44	31%
SIM	9/21	34/43	33%	7/20	37/44	31%
Season	Norton Bridge			Manampitiya		
	Dry	Not dry	OOB Error	Dry	Not dry	OOB Error
NEM	9/20	36/44	30%	13/23	33/41	28%
FIM	5/21	35/43	38%	8/21	35/43	33%
SWM	9/22	32/42	36%	5/16	34/43	39%
SIM	10/22	36/42	28%	16/25	34/39	22%

503

504

505

506

507

508

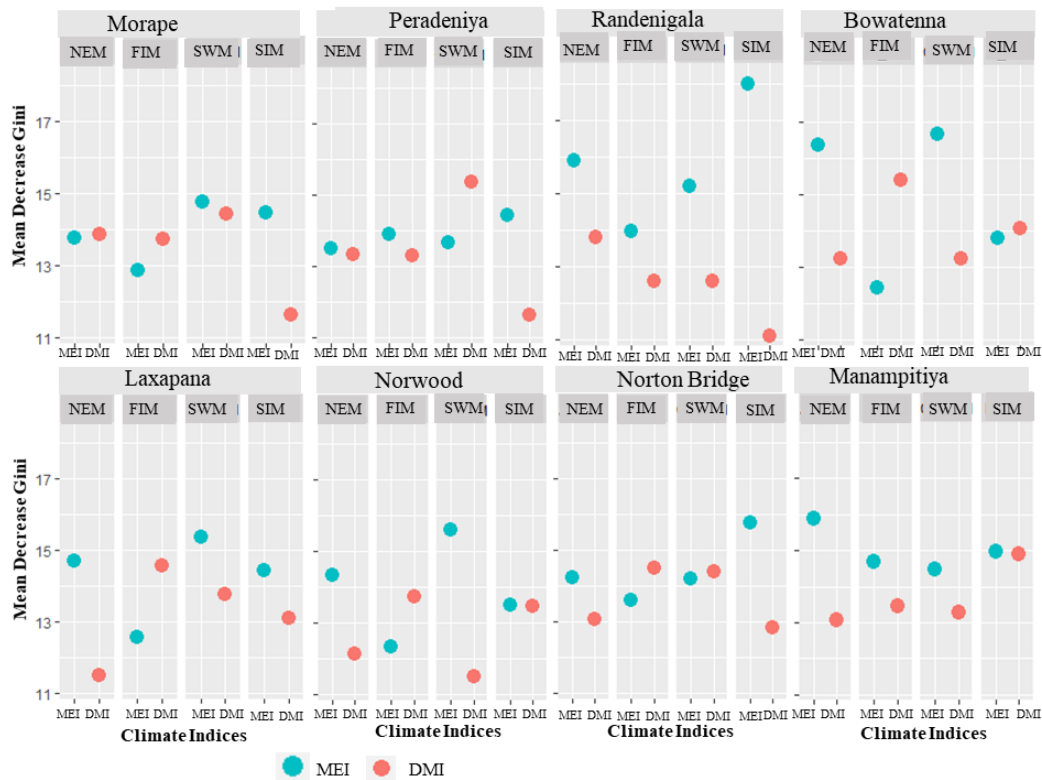
509

510



511

512



513

514 Figure A 7: Random forest importance of variable to identify the dry and not dry classes of rainfall anomalies

515